Structural Perturbation and Compensation by Directed Evolution at Physiological Temperature Leads to Thermostabilization of β-Lactamase†

Jochen Hecky and Kristian M. Müller*

Institut für Biologie III, Albert-Ludwigs-Universität, Schänzlestrasse 1, D-79104 Freiburg, Germany

Received February 1, 2005; Revised Manuscript Received June 9, 2005

ABSTRACT: The choice of protein for use in technical and medical applications is limited by stability issues, making understanding and engineering of stability key. Here, enzyme destabilization by truncation was combined with directed evolution to create stable variants of TEM-1 β-lactamase. This enzyme was chosen because of its implication in prodrug activation therapy, pathogen resistance to lactam antibiotics, and reporter enzyme bioassays. Removal of five N-terminal residues generated a mutant which did not confer antibiotic resistance at 37 °C. Accordingly, the half-life time in vitro was only 7 s at 40 °C. However, three cycles comprising random mutagenesis, DNA shuffling, and metabolic selection at 37 °C yielded mutants providing resistance levels significantly higher than that of the wild type. These mutants demonstrated increased thermoactivity and thermostability in time-resolved kinetics at various temperatures. Chemical denaturation revealed improved thermodynamic stabilities of a three-state unfolding pathway exceeding wild-type construct stability. Elongation of one optimized deletion mutant to full length increased its stability even further. Compared to that of the wild type, the temperature optimum was shifted from 35 to 50 °C, and the beginning of heat inactivation increased by 20 °C while full activity at low temperatures was maintained. We attribute these effects mainly to two independently acting boundary interface residue exchanges (M182T and A224V). Structural perturbation by terminal truncation, evolutionary compensation at physiological temperatures, and elongation is an efficient way to analyze and improve thermostability without the need for high-temperature selection, structural information, or homologous proteins.

Proteins, especially enzymes, have gained a central role in modern chemical, biotechnological, and biopharmaceutical industries. Thermostability and prolonged half-life times are the key general features desired besides the more case specific properties such as activity, catalytic specificity, enantioselectivity, or functional compatibility with organic solvents. A plethora of factors enhancing thermostability have been identified so far (*1*−*5*), for example, increased rigidity (*6*), better packing (*7*), fewer and smaller cavities (*8*, *9*), more hydrophobic residues in the protein core (*10*), and an increased number of van der Waals (*11*) and aromatic interactions (*12*). Higher thermostability can also be obtained by docking loops and chain termini to the protein core (*5*, *13*), backbone cyclization (*14*), additional disulfide bonds (*15*), introduction of metal-binding sites (*16*), and helix dipole stabilization (*17*). Comparative studies of thermophilic and mesophilic organisms revealed that thermostable proteins differ from their heat-labile counterparts by higher oligomerization states, reduced hydrophobic surface area, stronger intersubunit interactions, shortening or deletion of loop regions (*18*), increased helical content, and substitution of thermosensitive residues by more stable ones (*5*). The decreased backbone strain and the decreased number of glycines as well as the increased number of prolines enhance thermostability by reducing the entropy difference between the folded and the unfolded state (*19*). There is a growing body of evidence that improved hydrogen bonding and ionic interaction networks are the main factors determining the high thermostability of thermophilic proteins (*20*−*22*).

Although principle factors are known, a detailed understanding of thermostability still remains elusive (*23*). Today, computational, comparative, and evolutionary approaches work together to overcome the limits of current protein design knowledge. Computational redesign searching for a global minimum energy conformation (GMEC) has been used to generate mutants of the streptococcal protein G β1 domain, shifting the melting temperature from 83 to >100 °C (*24*), and of human growth hormone (hGH), increasing the melting temperature by 13−16 °C with 6−10 amino acid substitutions (*25*). The semirational "consensus concept" uses sequence alignments of homologous proteins to extract the most frequent residues at any position. On the basis of such alignments, a thermostable synthetic phytase was generated (*26*). Although computational and homology-guided design could be quite successful, they can only be applied when high-resolution structures or useful homologous sequences are available. In addition, genes for in silico-designed proteins need to be synthesized and proteins need to be characterized which can result in time-consuming cycles of design and testing.

† This work was supported by the DFG, Graduiertenkolleg 434 Biochemie der Enzyme.

* To whom correspondence should be addressed. Telephone: ++49-761-203-2748. Fax: ++49-761-203-2745. E-mail: kristian@biologie.uni-freiburg.de.

10.1021/bi0501885 CCC: $30.25
Published on Web 09/01/2005

In vitro or directed evolution is based on the principles that govern natural evolution, namely, (i) random mutagenesis, (ii) recombination, and (iii) screening or selection. Directed evolution uses iterative cycles of diversity generating steps, i and ii, followed by the identification of improved variants in a sieving step, iii, where the outcome of one cycle serves as the starting material of the subsequent cycle. Since recombination at the molecular level has been nicely demonstrated in the form of DNA shuffling (*27*, *28*) and added to the protein engineer's toolbox, enzymes have been improved considerably, for example, in terms of activity, selectivity, stability, and function in organic solvents (*29*).

The importance of the terminal regions of proteins for their structural or functional integrity has not been fully clarified. Terminal sections of homologous proteins often differ significantly in sequence and length, and are frequently poorly defined in crystal structures or not ordered at all (*30*). This could seemingly imply that terminal sequences of proteins are hardly relevant for protein structure and stability. According to the common view, conserved residues in highly homologous proteins contribute more to the overall stability of a molecule than residues with a rare occurrence at a specified position (*31*, *32*). However, screening the literature over the past two decades brings up a few reports drawing a more complex picture. The removal of several terminal residues can have various effects, including structural and folding defects, reduced conformational stability, a looser structure, and an enhanced susceptibility to proteolysis or aggregation. This has been demonstrated for, among others, RNase A (*33*), RNase HI (*34*), staphylococcal nuclease R (*35*), rhodanese (*36*, *37*), the Stoffel fragment of Taq DNA polymerase (*38*), chloramphenicol acetyl transferase (*39*), and the *exo small* β-lactamase of *Bacillus licheniformis* (*30*).

TEM lactamases are well-studied proteins. Currently, 21 X-ray structures are deposited in the Protein Data Bank (e.g., PDB entry 1tem, 1btl, 1axb, 1jwp, and 1fqg) which include a few high-resolution structures down to 0.85 Å (PDB entry 1m40). One part of the interest is due to the many mutations broadening the substrate spectrum of TEM lactamase and requiring the continuous improvement of lactam antibiotics. In this context, directed evolution has been used to predict future challenges (*40*). The catalytic activity has also been purposely applied for prodrug activation cancer therapy approaches in which TEM-l or a related lactamase was combined with antibodies (*41*, *42*). TEM lactamase has been a model for studying structure−function relationships (*43*, *44*). In addition, β-lactamase has been used as a marker enzyme for high-throughput assays and genome wide screens (*45*, *46*), and as a reporter in protein complementation assays (*47*, *48*).

Accordingly, we used β-lactamase as model enzyme and addressed the following questions: (i) How important are nonconserved terminal ends for protein function? (ii) Can the loss of seemingly essential parts be compensated? (iii) How can stability be achieved? (iv) To what extent can stability and activity be improved? (v) Do structural perturbation and compensation depend on each other? In short, our answers from our system are as follows: (i) Even a few nonconserved terminal residues can be essential for protein function. (ii) The loss of function due to a loss of terminal ends can be compensated with few mutations. (iii) Stabilization is achieved by strengthening small interaction clusters at domain boundaries. (iv) Stability and activity can be improved beyond those of the wild type. (v) Structural perturbation by truncation and compensating mutations act independently on protein stability.

Thus, structural perturbation in combination with directed evolution is a widely applicable, highly efficient tool for the analysis and generation of protein thermostability even in cases where no thermostable homologues and no three-dimensional structures are available. Our stabilized lactamases could prove to be useful for prodrug activation approaches, large-scale reporter enzyme assays, and protein complementation screens.

EXPERIMENTAL PROCEDURES

Plasmid Construction. TEM-1 β-lactamase deletion mutants NΔ3, NΔ5, CΔ1, and CΔ3 were generated by amplifying the TEM-1 gene from a pUC-derived plasmid (*49*) using the forward primers pr_sfi_pelB_DG_blawt (5′-TTACTCACGGCCCAGCCGGCCATGGCTGACGG**TCACCCAGAAACGCTGGTG**-3′; restriction sites are underlined and hybridizing regions are bold), pr_sfi_pelB_DG_bladelHPE (5′-TTACTCGCGGCCCAGCCGGCCATGGCTGAC-GGT**ACGCTGGTGAAAGTAAAAGATG**-3′), and pr_sfi_pelB_DG_bladelHPETL (5′-TTACTCACGGCCCAGCCGGCCATGGCTGACGGT**GTGAAAGTAAAAGATGCTGAAG**-3′) and the reverse primers pr_blawt_GG_his5_hind (5′-TAGTCAAGCTTACTAGTGATGGTGATGGTGGCCACC**CCAATGCTTAATCAGTGAGG**-3′), pr_bladelW_GG_his5_hind (5′-TAGTCAAGCTTACTAGTGATGGTGATGGTGGCCACC**ATGCTTAATCAGTGAGGCACC**-3′), and pr_bla_delKHW_GG_his5_hind (5′-TAGATCAAGCTTACTAGTGATGGTGATGGTGGCCACC**AATCAGTGAGGCACCTATCTC**-3′). The forward primers introduced a 5′ *Sfi*I restriction site, the C-terminal part of a pelB signal peptide (*50*), an aspartate-glycine linker, and the respective N-terminal modification (truncation) of the TEM-1 variants. The reverse primers introduced the modified TEM-1 C-termini, a biglycine linker, a pentahistidine tag, two stop codons, and a *Hin*dIII restriction site. The PCR products were digested with *Sfi*I and *Hin*dIII (NEB), isolated, and cloned into the *Sfi*I−*Hin*dIII fragment of pKMENGRbla (provided by K. M. Müller, unpublished), a derivative of the expression plasmid pAK400 (*51*) which carries a chloramphenicol resistance gene. The resulting pKJE_Bla-ΔN/C series of plasmids expressed the various TEM-1 genes under control of a *lac* promoter/operator region. Despite the constitutive expression of *lac*I on the plasmids, a strong phage T7g10 Shine-Dalgarno sequence (*52*) resulted in a relatively high basal gene expression level. Therefore, all selection steps were performed under stringent conditions without overexpression.

DNA Shuffling and Random Mutagenesis. Starting material for gene fragmentation of the mutant TEM-1 enzyme was generated by PCR using plasmid pKJE_Bla-NΔ5 and the oligonucleotides pr_sfi_pelB_DG_shuffl (5′-TTACTCACGGCCCAGCCGGCCATGGCTGACGG-3′) and pr_GG_his5_hind_shuffl (5′-TAGTCAAGCTTACTAGTGATGGTGATGGTGGCCACC-3′) which were homologous to the constant regions flanking the truncated β-lactamase gene. *Taq* DNA polymerase (Sigma) was used in all amplification and reassembly steps. Approximately 4−4.5 μg of PCR

product was randomly digested using 0.2 unit of DNase I (Sigma) in a total volume of 50 μL of 50 mM Tris-HCl (pH 7.5) and 1 mM $MgCl_2$ for 12 min at 25 °C. Reactions were stopped by adding 4 μL of 0.5 M EDTA and stored on ice. DNA fragments were analyzed on 2% (w/v) agarose gels, and fragments of ~50−150 bp were excised and purified using the QiaexII gel extraction kit (Qiagen). Approximately 100−300 ng of the isolated fragments was assembled in a primer extension reaction without added primers. The reaction mix contained 2.5 units of *Taq* DNA polymerase (Sigma), each dNTP at 0.4 mM (Amersham-Pharmacia), and 2 mM $MgCl_2$ in the supplied buffer (Sigma). Assembly reactions were carried out in a thermocycler (Eppendorf) using the following program: 94 °C for 3 min; 10 cycles comprising 1 min at 94 °C, 1 min at 45 °C with a 0.3 °C increase per cycle, 1 min at 72 °C, and one step of 5 min at 72 °C; 15 cycles of 1 min at 94 °C, 1 min at 50 °C with a 0.4 °C increase per cycle, 1 min at 72 °C, and one step of 5 min at 72 °C; 10 cycles of 1 min at 94 °C, 1 min at 56 °C with a 0.5 °C increase per cycle, 1 min at 72 °C, and one step of 5 min at 72 °C; and 10 cycles of 1 min at 94 °C, 2 min at 61 °C with a 0.5 °C increase per cycle, 2 min at 72 °C, and an additional 5 min at 72 °C. To introduce additional mutations and to make sure that all assembled genes contained 5′ *Sfi*I and 3′ *Hin*dIII restriction sites for subsequent cloning, $^1/_5$ volume of the assembly PCR mixture was amplified in an error-prone PCR using the primers pr_sfi_pelB_DG_shuffl and pr_GG_his5_hind_shuffl at a final concentration of 0.5 μM each. The reaction mixture included 7 mM $MgCl_2$, 0.5 mM $MnCl_2$, each dNTP at 0.4 mM, and 2.5 units of *Taq*. The program used was 3 min at 94 °C, 25 cycles of 1 min at 94 °C, 1 min at 68 °C, and 1 min at 72 °C, and a final step of 7 min at 72 °C. The PCR products were purified using the GFX PCR DNA and Gel Band Purification Kit (Amersham-Pharmacia), digested with *Sfi*I and *Hin*dIII, and cloned into the pKJE_Bla-NΔ5 vector treated with the same enzymes.

The DNA shuffling and random mutagenesis procedures in combination with in vivo selection steps were used to perform three rounds of directed evolution. Clones that were selected were pooled and served as templates for subsequent rounds. In the last round of directed evolution, the error-prone PCR step following DNA shuffling was replaced by a standard PCR procedure to prevent the introduction of deleterious mutations into the recombined clones.

In Vivo Selection in Liquid Culture and on Plates. Plasmid mutant libraries S1 to S3 of pKJE_Bla-NΔ5 were butanol precipitated (*53*) and transformed in 100 μL aliquots of electrocompetent *Escherichia coli* XL-1 Blue cells using a Bio-Rad gene pulser (1.7 kV, 200 Ω, 25 μF). After transformation, 900 μL of 2YT containing 2.5 mM KCl and 10 mM $MgCl_2$ was added and the cell suspensions were incubated in 10 mL glass test tubes for 60−70 min at 37 °C with orbital shaking. Transformation efficiency was assessed by plating 50 μL of each transformation mixture on LB/Cm plates (1% bactotryptone, 0.5% yeast extract, 0.5% NaCl, 25 μg/mL chloramphenicol, and 1.5% agar). For survival screening, LB/Cm plates were supplemented with adjusted concentrations of ampicillin.

From the first transformation, 100 μL aliquots were used to inoculate 8 × 6 mL of LB/Cm in test tubes with 20 μg/mL (five samples), 40 μg/mL (one sample), and 60 μg/mL (one sample) ampicillin. As growth was observed in only one of seven samples containing ampicillin after 50 h, three additional transformations were carried out and transferred to 24 mL of LB/Cm with 20 μg/mL ampicillin using 100 mL Erlenmeyer flasks. After being shaken for 50 h at 37 °C and 200 rpm, two of three cultures grew. The long incubation times that were required indicated that cultures started from single cells. Individual clones were obtained by plating aliquots on LB/Cm agar with 20 μg/mL ampicillin and sequenced. XL-1 Blue cells transformed with any of the three plasmids that were obtained were plated on 50, 100, and 200 μg/mL ampicillin, exhibiting growth of two clones at 50 μg/mL and one at 100 μg/mL. Thus, the selection level for the subsequent round was set to 100 μg/mL ampicillin. For the second round, 950 μL of the transformation was sedimented by centrifugation (2 min at 2000*g*), resuspended in approximately 250 μL of 2YT, and plated on 14.5 cm LB/Cm agar plates with 100 μg/mL ampicillin. After incubation for 18 h at 37 °C, all cells were pooled by resuspending them in LB/Cm. Approximately 2000 cells from this mixture were spread on dishes containing up to 175 μg/mL ampicillin to determine the next selection level, which was set to 200 μg/mL. Additionally, a 4 mL sample of the pooled cells was taken to isolate plasmid DNA which was used as parental DNA for the third round of directed evolution. For the third round, six transformation mixtures were treated as in the former round.

Protein Expression and Purification. For the expression of the β-lactamase mutants directed to the periplasm, the pKJE vector series was transformed in BL21 cells. Overnight cultures in 2YT with 25 μg/mL chloramphenicol (2YT/Cm) were inoculated from glycerol stocks and grown at 28 °C for ~16−18 h. Expression cultures of 4 × 1 L of 2YT/Cm were inoculated with a start OD_{600} of 0.15 and grown at 24 °C for NΔ5-clone,[1] and at 25−30 °C for all other constructs. Expression was induced at an OD_{600} of 0.7 with 0.5 mM IPTG (isopropyl β-D-thiogalactoside). Forty minutes after induction, cultures were supplemented with 100 μg/mL ampicillin to select for β-lactamase-producing cells. Cultures were harvested after 4−5 h at an OD of 4−5 at 6000*g* in a GS-3 rotor (Sorvall). Pellets from 1 L of culture were pooled in 50 mL polypropylene tubes and stored at −80 °C. For purification, one pellet was resuspended in phosphate buffer [50 mM sodium phosphate and 500 mM NaCl (pH 7.0)] with 200 units of benzonase (Sigma). Two pH values (7.0 and 7.2) were tested with equal results. Cells were disrupted in a French press (700 bar, five to six cycles in a precooled cell). Samples were held on ice whenever possible. The crude cell extract was clarified by centrifugation [41000*g*, SS-34 rotor (Sorvall), 4 °C] and filtration [0.45 μm PES syringe filters (Roth)]. An ÄKTA purifier (Amersham-Pharmacia) was used for chromatography monitoring A_{254} and A_{280}. Phenylboronate affinity chromatography was the first purification step for all enzyme variants; 2 mL columns (MoBiTec) were equilibrated, loaded, and finally washed with phosphate buffer until A_{280} approached baseline. β-Lactamase

[1] Abbreviations: wt-clone, wild-type β-lactamase construct directed to periplasm; wt-clone-cyt, wt-clone directed to cytosol; NΔ5-clone, β-lactamase truncated by five N-terminal residues; NΔ5-S3/6 and NΔ5-S3/7, optimized deletion mutants 6 and 7, respectively; FL-S3/6, full-length β-lactamase with substitutions of mutant 6; FL-S3/6-cyt, full-length β-lactamase with substitutions of mutant 6 directed to cytosol; Cm, chloramphenicol.

variants were eluted with 0.5 M borate and 0.5 M NaCl (pH 7.0). The second purification step for the His-tagged enzymes was immobilized metal ion affinity chromatography (IMAC) with a 4 mL Ni−NTA superflow matrix (Qiagen) in a C 10/10 column (Amersham-Pharmacia) equilibrated with phosphate buffer containing 5 mM imidazole in some cases. Enzymes were purified and eluted with a step gradient (5, 10, 16, and 100%) of 50 mM sodium phosphate, 0.25 M imidazole, and 0.5 M NaCl (pH 7.0). Protein samples were dialyzed for further characterization against 3 × 1 L of 50 mM sodium phosphate and 150 mM NaCl (pH 7.2, ≥8 h) containing additionally 1 mM EDTA in the first dialysis.

In the case of wt-clone and NΔ5-S3/6, IMAC-purified and dialyzed samples were contaminated (20−50%) with their unprocessed forms. In these cases, hydrophobic interaction chromatography (HIC) was used to separate the mature from the more hydrophobic unprocessed form using a 1 mL phenyl-Superose HR 5/5 column (Amersham-Pharmacia) equilibrated with 1 M $(NH_4)_2SO_4$. NΔ5/S3-6 samples were supplemented with ammonium sulfate crystals to a final concentration of 1 M $(NH_4)_2SO_4$, cleared by centrifugation (10 min, 27000*g*, 4 °C, SS-34 rotor) and filtration (0.45 μm syringe filter). A 0 to 100% linear gradient (30 mL) of 25 mM sodium phosphate and 75 mM NaCl (pH 7.2) was applied. For wt-clone, HIC was applied following phenylboronate chromatography. Because of protein precipitation, only 0.65 M ammonium sulfate was added. The unprocessed form was retained on the column, while the mature enzyme was in the flow-through. A final IMAC purification was carried out as described above.

Cytoplasmatically expressed β-lactamase variants wt-clone-cyt and FL-S3/6-cyt were purified by phenylboronate affinity chromatography and IMAC as described. To further increase purity for biophysical characterization, an additional anion exchange chromatography was carried out. Samples were dialyzed [25 mM Tris-HCl and 25 mM NaCl (pH 8.0)], loaded on a Mono Q HR 5/5 column (Amersham-Pharmacia), and eluted with a 0 to 100% linear gradient (30 mL) of 25 mM Tris-HCl and 0.5 M NaCl (pH 8.0). The eluted protein was dialyzed against phosphate buffer.

Purity was assessed by SDS−12.5% polyacrylamide gel electrophoresis followed by Coomassie staining. For biophysical characterizations, the purity of the processed form of mutants was better than 90%. The purity and percent unprocessed protein were quantified from scanned Coomassie-stained gels using the image analysis software Scion/NIHimage. Amino acid compositions of all variants were confirmed by electrospray mass spectrometry within typical deviations from calculated masses. Enzymes were characterized within 1 week of purification. Before being used, enzyme solutions were clarified by centrifugation (30 min, 15000*g*, 10 °C). Protein concentrations were taken from absorbance spectra at 280 nm. Molar extinction coefficients were calculated according to the method of Gill and von Hippel (*54*).

Enzyme Assays. The kinetic parameters of the β-lactamase variants were assayed photospectrometrically at 486 nm using the chromogenic substrate nitrocefin ($\Delta\epsilon_{486} = 16\,000\ M^{-1}\ cm^{-1}$) and an Ultrospec 3000 spectrophotometer (Amersham-Pharmacia) (*55*). Routinely, 20 μL of the enzyme solution was added to 980 μL of nitrocefin mix [0.2 mM nitrocefin, 50 mM potassium phosphate, and 0.5% DMSO (pH 7.0)]. Measurements were repeated at least twice, and standard deviations were calculated.

K_M values were obtained by measuring initial rates with substrate concentrations ranging from 10 to 500 μM and enzyme concentrations of 2.7−5.9 nM for NΔ5-clone and 0.5 nM for all other mutants. Data were fitted to the Michaelis−Menten equation using the Marquardt−Levenberg algorithm implemented in SigmaPlot (SPSS). Thermoactivity was probed by preparing a 292 nM solution for NΔ5-clone and 25 nM solutions for all other variants, which were split into three aliquots. The first aliquot was incubated for 5 min at a given temperature (25−70 °C) in a heated water bath, while both of the remaining samples were held on ice. The sample was mixed by short vortexing; 20 μL was transferred to 980 μL of nitrocefin mix preheated to the respective assay temperature, and the initial reaction rate was determined between 5 and 25 s in a heated spectrophotometer. The second aliquot was preheated for 30 s at the respective temperature, while the third aliquot was assayed after incubation on ice for 10 min.

The enzyme decay was fitted using the three-parameter exponential decay fit implemented in SigmaPlot:

$$\frac{\Delta A}{\Delta t} = a + \left[\frac{\Delta A}{\Delta t}\right]_0 e^{-\lambda t}$$

where *a* is a parameter accounting for basal and accumulated absorption of the nitrocefin solution and $T_{1/2} = \ln 2/\lambda$.

Urea-Induced Unfolding and Data Analysis. Unfolding of the β-lactamase variants was evaluated by fluorescence spectroscopy using a FluoroMax-2 (Jobin-Yvon) or a RF-1502S (Shimadzu) spectrofluorimeter, respectively. The red shift of λ_{max} of fluorescence intensity as a function of urea concentration was monitored; 300−400 nM enzyme solutions [50 mM sodium phosphate and 150 mM NaCl (pH 7.2)] containing 0.25−8 M urea were equilibrated for 18−20 h at 19 °C. Fluorescence emission spectra were recorded from 320 to 380 nm at 20−23 °C while exciting at 280 nm. For each data point, four scans were averaged. If necessary, fluorescence spectra were corrected for the background fluorescence of the solution (buffer and denaturant). Using SigmaPlot, a tricube weight function (Loess; sampling proportion of 0.25, polynomial degree of 3) was applied to smooth fluorescence intensity spectra to obtain the associated λ_{max} values.

The measured fluorescence data were evaluated assuming a three-state N ⇌ I ⇌ U model with two equilibrium constants, K_{NI} and K_{IU}. The emission maximum (y_{obs}) as a function of denaturant concentration ([D]) was deconvoluted in the constituting signals of the three conformational states (y_N, y_I, and y_U) according to their fraction present (f_N, f_I, and f_U), which is described by $y_{obs} = y_N f_N + y_I f_I + y_U f_U$ (*56*). The law of mass action ($K_{NI} = [I]/[N]$, $K_{IU} = [U]/[I]$) was combined with mass conservation ($[N]_0 = [N] + [I] + [U]$) to calculate the fractions [$f_N = 1/(1 + K_{NI} + K_{NI}K_{IU})$, $f_I = K_{NI}/(1 + K_{NI} + K_{NI}K_{IU})$, and $f_U = K_{NI}K_{IU}/(1 + K_{NI} + K_{NI}K_{IU})$]. Thermodynamic parameters were introduced using the linear extrapolation method based on the relation $\Delta G^\circ = -RT \ln K = \Delta G^\circ_{H_2O} - m[D]$ assuming a linear dependence for all states (*57*). Thus, the parameters $\Delta G^\circ_{NI,H_2O}$, $\Delta G^\circ_{IU,H_2O}$, m_{NI}, m_{IU}, and y_I were fitted to the fluorescent data using the equation

$$y_{obs} = \frac{y_N + y_I e^{(-\Delta G^\circ_{NI,H2O} + m_{NI}[D])/RT} + y_U e^{(-\Delta G^\circ_{NI,H2O} + m_{NI}[D])/RT} \times e^{(-\Delta G^\circ_{IU,H2O} + m_{IU}[D])/RT}}{1 + e^{(-\Delta G^\circ_{NI,H2O} + m_{NI}[D])/RT} + e^{(-\Delta G^\circ_{NI,H2O} + m_{NI}[D])/RT} \times e^{(-\Delta G^\circ_{IU,H2O} + m_{IU}[D])/RT}} \quad (1)$$

where y_N and y_U were set to the average of the first and last data points, respectively. A slope in the baselines was not seen. To account for small changes between the absolute maxima measured with the two fluorimeters, the normalized fraction unfolded [$f_{unfold} = (y_{obs} - y_F)/(y_U - y_F)$] is given in the plot. The midpoints of transitions are given by

$$[D]_{1/2} = \Delta G^\circ_{H_2O}/m \quad (2)$$

RESULTS

Generation and in Vivo Characterization of Four β-Lactamase Deletion Mutants. Class A β-lactamases (EC 3.5.2.6) are bacterial periplasmic enzymes with relatively diverse amino acid sequences and stabilities but very similar tertiary structures (*58*). The polypeptide backbones of class A β-lactamases superimpose very well in the core (active site) region (Figure 1a), but the ends of the terminal helices differ in terms of amino acid composition, length, and conformation (Figure 1a,b). To investigate how these variable terminal regions influence activity as a result of folding and stability, four deletion mutants of TEM-1 β-lactamase were created lacking either the first three (NΔ3) or five (NΔ5) N-terminal residues or one (CΔ1) or three (CΔ3) C-terminal residues. The design of the deletions was based on structural alignments, our own experiments (not shown), and previous random mutagenesis studies (*43*). The first three residues at the N-terminus (His, Pro, and Glu) have high temperature factors (up to 23.8 Å^2, average of 13.1 Å^2) and solvent accessibilities (PDB entry 1btl), and their deletion was expected to affect stability only marginally. The NΔ5 truncation (named NΔ5-clone) included the adjacent threonine and leucine, the first of which is nearly completely buried and forms an H-bond with Ser285 of the C-terminal helix. At the C-terminal end, only one or three residues were removed as the distal tryptophan has been shown to be "essential" in a previous study (*43*). The plasmids were designed to encode either the mature wild-type β-lactamase (named wt-clone) as a reference or the respective deletion mutants as fusion proteins with an N-terminal pelB periplasmic targeting sequence, an aspartate-glycine tag to ensure an equally efficient processing rate for the variants differing in their N-termini, and a C-terminal His tag for purification (Figure 1c).

A Petri dish growth assay examined the extent to which terminal truncation affected the in vivo functionality of TEM-1 β-lactamase (Figure 2a). Colony numbers of cells producing any of the deletion mutants decreased significantly when the selective pressure increased from 0 to 50 μg/mL ampicillin at 37 °C. For the mutants NΔ5-clone and CΔ3-clone, no colonies were observed after incubation for 40 h, suggesting an important role for the terminal residues.

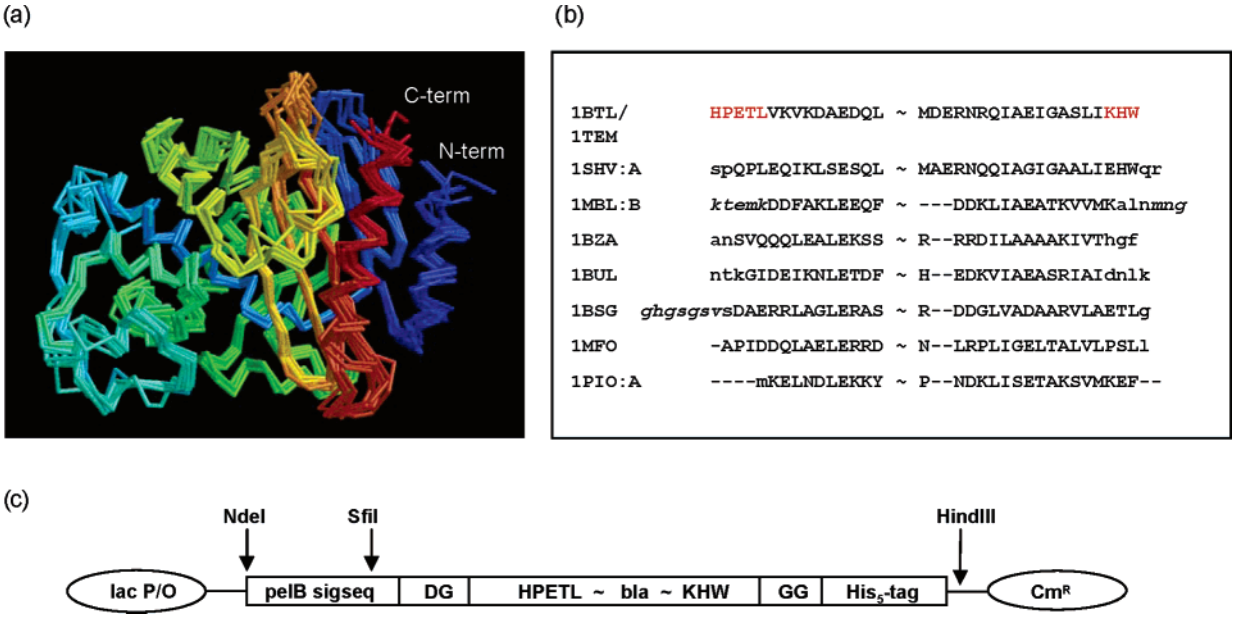

FIGURE 1: (a) Structural superposition of C_α traces of various β-lactamases from different bacterial species using the CE algorithm (*82*). Contiguous secondary structural elements are colored sequentially from blue at the N-terminus to red at the C-terminus using RasMol (*83*). (b) Structure-based sequence alignment of the N- and C-terminal parts of the β-lactamases displayed in panel a. Only sequences corresponding to the N-terminal and C-terminal helix of the TEM-1 enzyme (PDB entries 1btl and 1tem) are shown. The sequences are specified by their respective PDB codes given on the left. Lowercase letters represent residues that were ignored by the CE algorithm and therefore are not included in the structural superposition. Italic letters denote residues present in the sequence files deposited in the Swissprot database but missing in the corresponding X-ray structure. Omitted parts of the sequence in the middle of the panel are symbolized by ~. The selected β-lactamase genes showed levels of homology ranging from 67.8 to 32.4%. The corresponding structures had rmsd values ranging from 1.2 to 2.2 Å (with reference to the TEM-1 β-lactamase) and *Z*-scores above 7. The structural superposition demonstrates the structural variability of the terminal helices. (c) Design of the expression vectors. A pelB signal sequence was linked by aspartate and glycine to the coding region of mature TEM β-lactamase. A His_5 tag separated by two glycine residues was fused to the C-terminus to ease purification. All plasmids contained a chloramphenicol resistance gene. Important endonuclease restriction sites are indicated. In the case of the cytoplasmatically expressed variants, the pelB signal sequence and the aspartate-glycine residues were replaced with a single methionine residue.

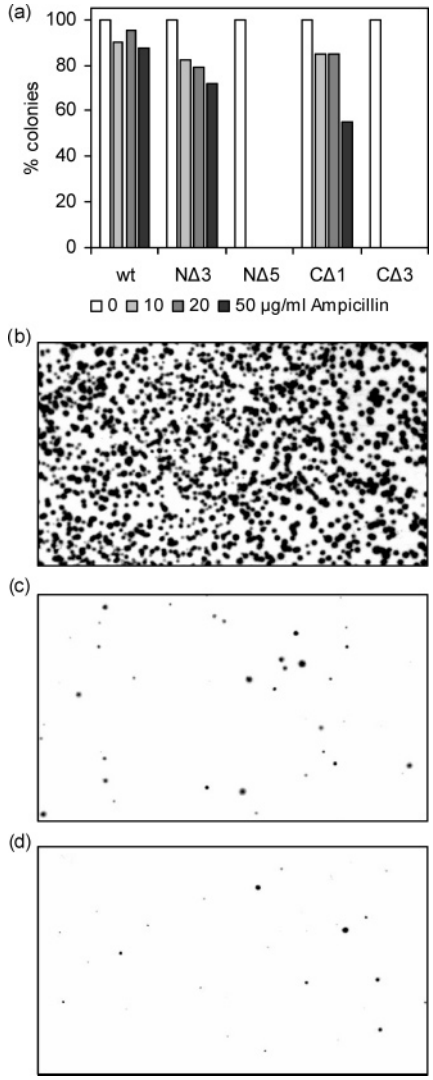

FIGURE 2: (a) In vivo fitness of initially generated β-lactamase deletion mutants. Approximately 3500 freshly transformed XL-1 Blue cells carrying the respective plasmid were selected on LB agar plates containing chloramphenicol and 10−50 μg/mL ampicillin or chloramphenicol alone (100% clones). Plates were analyzed after incubation for 20 h at 37 °C. For NΔ5-clone and CΔ3-clone, no colonies could be observed in the presence of ampicillin. (b−d) Photographs of colonies of optimized NΔ5-β-lactamase deletion mutants on LB agar plates containing 0 (b), 350 (c), or 700 μg/mL ampicillin (d). Approximately 1500 cells of a regrown culture of pooled colonies isolated in the third round of directed evolution were plated. Plates were photographed after 20 h (b) or after incubation for 40 h at 37 °C (c and d).

To test for residual activity which might have been obscured under stringent selection conditions that were applied (basal gene expression, growth at 37 °C, selection on plate), growth was also assayed with induction and in liquid culture. With induction cells grew on plates with up to 50 μg/mL ampicillin at 25 °C and in liquid culture with optimal aeration also at 37 °C. This suggested that both truncations induced structural perturbations but at the same time allowed for folding into active states. NΔ5-clone conferred resistance to a much lower extent than CΔ3-clone and was therefore chosen for subsequent optimization. In vivo, the shortened enzyme may suffer from rapid thermal inactivation, aggregation, and/or accelerated degradation. Thus, in vitro experiments were used to gain a more focused picture.

Directed Evolution of β-Lactamase Deletion Mutant NΔ5. Impaired truncation mutant NΔ5-clone was revitalized by three rounds of directed evolution comprising random mutagenesis by error-prone PCR and DNA shuffling of a PCR product. The ability to confer resistance to increasing amounts of antibiotic on plates or liquid culture at 37 °C was the only selection criterion. In three successive rounds, $\sim 19 \times 10^3$, $\sim 147 \times 10^3$, and $\sim 260 \times 10^3$ clones were generated and screened for survival on plates containing 20, 100, and 200 μg/mL ampicillin, respectively, giving rise to 3, 600, and approximately 7000 colonies, respectively.

Table 1 summarizes all sequenced clones isolated in the course of directed evolution sorted by shuffling round (S1−S3). Additionally, the table includes relative solvent accessibilities and average side chain atomic temperature factors (taken from PDB entry 1btl) (*59*) for each of the substituted wild-type residues. The five clones sequenced after the second optimization round shared two mutations, M182T and T265M [numbering from Ambler et al. (*60*)], which were already present after the first round.

After the final optimization step, the library was pooled and the maximum level of ampicillin resistance was determined on plates (Figure 2b−d). Normal colony development of a significant number of clones was seen up to 700 μg/mL, and after prolonged incubation times of 40 h, clones could even be detected at 1000 μg/mL. In contrast, the wild-type construct did grow only up to 500 μg/mL. Twenty-six clones were picked from the 800−1000 μg/mL plates and sequenced. The 26 sequences corresponded to 15 individual clones (Table 1). All clones shared two mutations, M182T and A224V. The M182T mutation has previously been demonstrated to compensate for folding defects (*61*) and stability losses (*62*, *63*). The second mutation (A224V) prevailed at the increased selective pressure of the third round and has to our knowledge not been studied before.

Both mutations are at least 17 Å from the site of deletion, indicating independent compensation of the structural interference imposed by deletion. Figure 3 highlights the most frequently mutated residues mapped to the known tertiary structure of TEM-1 β-lactamase. In general, the sets of mutations found in individual optimized variants were always scattered throughout the entire structure and never clustered adjacent to the site of deletion.

Construction of Full-Length Mutants, Cytosolic Expressed Variants, and Protein Purification. Optimized clone NΔ5-S3/6 was re-elongated to elucidate the extent to which the set of mutations compensating for protein destabilization upon terminal truncation affects the complete enzyme. The full-length clone named FL-S3/6 was constructed by adding the missing residues according to the schematic representation shown in Figure 1c. This variant was designed for translocation to the periplasm and was expressed in *E. coli* strains XL-1 Blue and RV308 to probe its functionality in vivo. Unexpectedly, the number of colonies on plates (20 h, 37 °C) containing chloramphenicol and ampicillin (100 μg/mL) was significantly lower (approximately 50%) than the number of colonies grown on control plates without ampicillin which was in contrast to NΔ5-S3/6 where almost all colonies survived (>98%). To distinguish between protein function and protein translocation, enzymatic activities of crude whole cell extracts of FL-S3/6 were tested relative to the nonextended mutant NΔ5-S3/6. No significant differences

Table 1: Amino Acid Substitutions (at given positions) Selected in the Course of Directed Evolution of the NΔ5 Deletion Mutant[a]

	31	37	38	42	52	56	59	63	82	84	88	96	104	120	147	150	153	159	168	177	182	192	195	198	206	208	224	240	247	256	265	277
wild-type	V	E	D	A	N	I	S	E	S	I	Q	H	E	R	E	A	H	V	E	E	M	K	T	L	Q	I	A	E	I	K	T	R
% acc	63.3	15.1	55.7	18.0	84.3	45.8	28.7	66.3	24.0	19.1	59.9	68.2	66.3	47.4	50.1	40.1	51.1	25.9	54.2	48.1	20.3	36.0	45.5	40.7	25.6	18.5	27.5	56.5	0	73.1	4.7	60.8
B-factor (sc)	8.3	12.2	19.9	11.6	16.7	8.7	11.0	25.5	8.8	13.8	33.5	20.7	34.1	25.0	20.6	8.3	16.5	6.5	21.1	23.5	7.9	12.1	14.6	25.7	14.0	13.8	8.2	26.1	5.4	26.0	7.0	30.9
S1/1																			A		**T**										M	
S1/2													G								**T**		**S**				**V**			R		
S1/3																	**R**												V			
S2/1																	**R**				**T**				H		**V**				M	
S2/2															G					K	**T**										M	
S2/3																					**T**										M	
S2/4																			A		**T**	E	**S**				**V**				M	
S2/5				G																	**T**										M	
S3/1 (×2)					S					**V**					G				V		**T**						**V**					
S3/2 (×4)														G			**R**	A			**T**						**V**					
S3/4 (×3)		D										Y									**T**						**V**				M	
S3/5 (×4)	A													G							**T**						**V**		V			
S3/6																	**R**				**T**		**S**				**V**					
S3/7 (×3)							G			**V**											**T**		**F**				**V**		V			
S3/17										**V**											**T**						**V**					
S3/18										**V**							**R**				**T**		**S**				**V**					
S3/19														G							**T**						**V**	G			M	K
S3/20	A		N	G					F	**V**											**T**		**S**	P			**V**		V	R	M	
S3/21	A																**R**				**T**		**S**				**V**					
S3/22									E		E						**R**		A		**T**						**V**			R		
S3/23					D			K		**V**						T	**R**				**T**		**S**	P			**V**					
S3/24						T				**V**							**R**				**T**					M	**V**					
S3/26																	**R**				**T**					M	**V**					
	31	37	38	42	52	56	59	63	82	84	88	96	104	120	147	150	153	159	168	177	182	192	195	198	206	208	224	240	247	256	265	277

[a] Amino acid substitutions of the selected deletion mutants are shown with regard to the wild-type sequence. Residues are numbered according to the method of Ambler et al. (*60*). Mutants are grouped according to the round of directed evolution in which they were selected (S1−S3). The frequency of individual selected clones containing the same set of mutations is shown in parentheses. The most prevalent amino acid substitutions of the third round mutants are shown in bold type. % acc is the relative solvent accessibility, the ratio between calculated and vacuum accessibility expressed as a percentage using What If (*72*). *B*-factors corresponding to the average of side chain atoms were calculated from the data given in the Protein Data Bank (PDB entry 1btl).

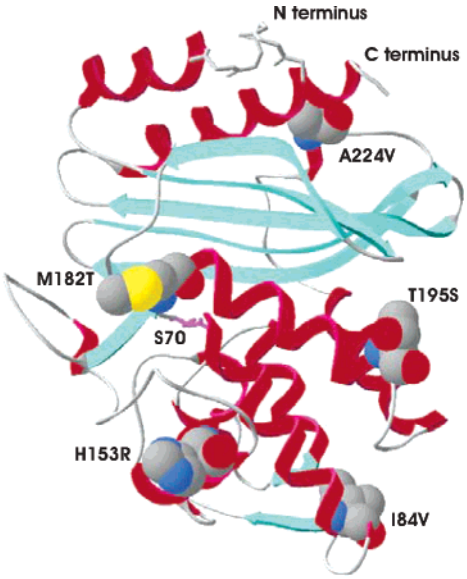

FIGURE 3: Ribbon representation of wild-type TEM-1 β-lactamase (PDB entry 1btl). The N- and C-termini are indicated. Residues most frequently mutated are shown as full atoms (e.g., M182T). The catalytic serine residue (S70) is colored magenta. Amino acids are numbered according to the system of Ambler (*60*). Most of the mutated amino acid residues are located near the protein surface. The figure was drawn using Swiss PDB viewer (*84*).

in hydrolase activity with the chromogenic substrate nitrocefin were seen, hinting that enzyme translocation could be the main reason. In agreement with these data, weakened cleavage of the signal sequence of clone FL-S3/6 was also observed in the purification process (see below). Consequently, a cytosolic expressed variant was cloned (FL-S3/6-cyt) by replacing the signal sequence and the Asp-Gly tag with a methionine start codon. To ensure correct biophysical comparisons, the analogous construct for wild-type lactamase (wt-clone-cyt) was cloned.

The generated β-lactamase variants (wt-clone periplasmatic, wt-clone-cyt, NΔ5-clone, optimized mutants NΔ5-S3/6 and NΔ5-S3/7, and FL-S3/6-cyt) were expressed at 24 °C to 30 °C and purified. Two purification steps were primarily applied: (1) a substrate analogue affinity chromatography using phenylboronate and (2) an immobilized metal ion affinity chromatography. This purification procedure worked very well for deletion mutant NΔ5-clone (Figure 4) and optimized mutant NΔ5-S3/7. However, significant amounts of unprocessed protein after the first purification step were seen on gels in the case of wt-clone (approximately 30% unprocessed form), mutant NΔ5-S3/6 (approximately 50%), and FL-S3/6 periplasmatic (approximately 65%). The identity of the protein forms was verified by mass spectrometry. For biophysical studies, additional purification steps were applied (see Experimental Procedures).

Kinetic Constants, Thermoactivity Profiles, and Half-Life Times. Kinetic constants were determined spectrophotometrically at 25 °C using the colorimetric substrate nitrocefin (Table 2). The Michaelis constant (K_M) of NΔ5-clone approximated that of wt-clone, but the turnover number (k_{cat}) decreased ~6-fold, implying an active site organization sufficient for binding but not for effective catalysis.

To test and compare the temperature dependency of activity and the kinetics of heat-induced inactivation, a thermoactivity screen was conducted with most variants

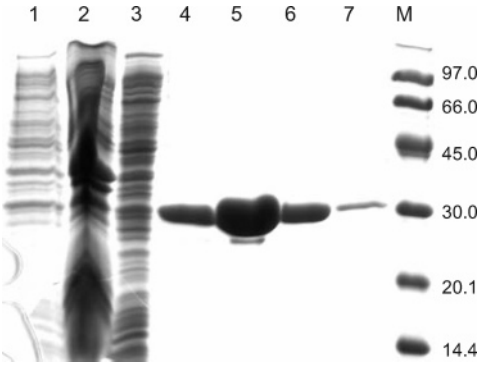

FIGURE 4: Expression and purification of the initial β-lactamase deletion mutant (NΔ5-clone). Coomassie-stained SDS−12.5% polyacrylamide gel of samples collected before and after purification by phenylboronate (PheBo) and immobilized metal ion affinity chromatography (IMAC), respectively: lane 1, whole cells before induction; lane 2, whole cell lysate after induction; lane 3, disrupted cell supernatant; lanes 4−7, fractions of IMAC elution peak; and lane M, molecular mass markers. The molecular masses (kilodaltons) of the individual marker bands are given.

Table 2: Kinetic Parameters[a]

β-lactamase variant	k_{cat} (s^{-1})	K_M (μM)	k_{cat}/K_M (M^{-1} s^{-1})
wt-clone	780 ± 9	84.4	9.24×10^6
NΔ5-clone	123 ± 2	61.0	2.02×10^6
NΔ5-S3/6	728 ± 7	58.9	12.4×10^6
NΔ5-S3/7	732 ± 19	64.3	11.4×10^6
wt-clone-cyt	602 ± 8	52.2	11.5×10^6
FL-S3/6-cyt	633 ± 9	70.6	8.97×10^6

[a] Kinetic constants were determined at 25 °C in 50 mM potassium phosphate buffer and 0.5% DMSO (pH 7.0) using the β-lactam compound nitrocefin as the substrate.

purified. In these experiments, turnover rates were assayed at increasing temperatures (25−70 °C) after specific incubation times (Figure 5).

The thermoactivity profiles of wt-clone varied clearly depending on the pretreatment (Figure 5a). The temperature optimum after ice incubation and preheating of 30 s at the assay temperature was 40 °C. However, when the enzyme was preheated for 5 min, the maximum shifted down to 35 °C, indicating the beginning of thermal unfolding.

Truncated NΔ5-clone maintained its highest activity at 25 °C, the lowest temperature that was examined (Figure 5b). With increasing temperatures, enzyme activity dropped rapidly and approached zero at 40 °C. A detailed analysis of the reaction rate at 40 °C following incubation on ice showed that this mutant was heat inactivated during the measurement within seconds of addition to the preheated assay mixture (Figure 6a). The observed decrease in the reaction rate over time could be fitted by an exponential decay equation yielding a half-life time of 7 s at 40 °C (Figure 6b).

The 0 and 30 s temperature−activity profiles of optimized mutant NΔ5-S3/6 (Figure 5c) largely resembled those of wt-clone. However, the 5 min preheating profile differed significantly. The temperature−activity curve of this optimized mutant was shifted to higher temperatures by ~8 °C compared to that of wt-clone (Figure 5a,f).

The full-length optimized mutant FL-S3/6-cyt (Figure 5d) exhibited thermostability features superior to those of optimized deletion mutant NΔ5-S3/6 and the corresponding wt-clone-cyt (Figure 5e,f). The catalytic activities of these

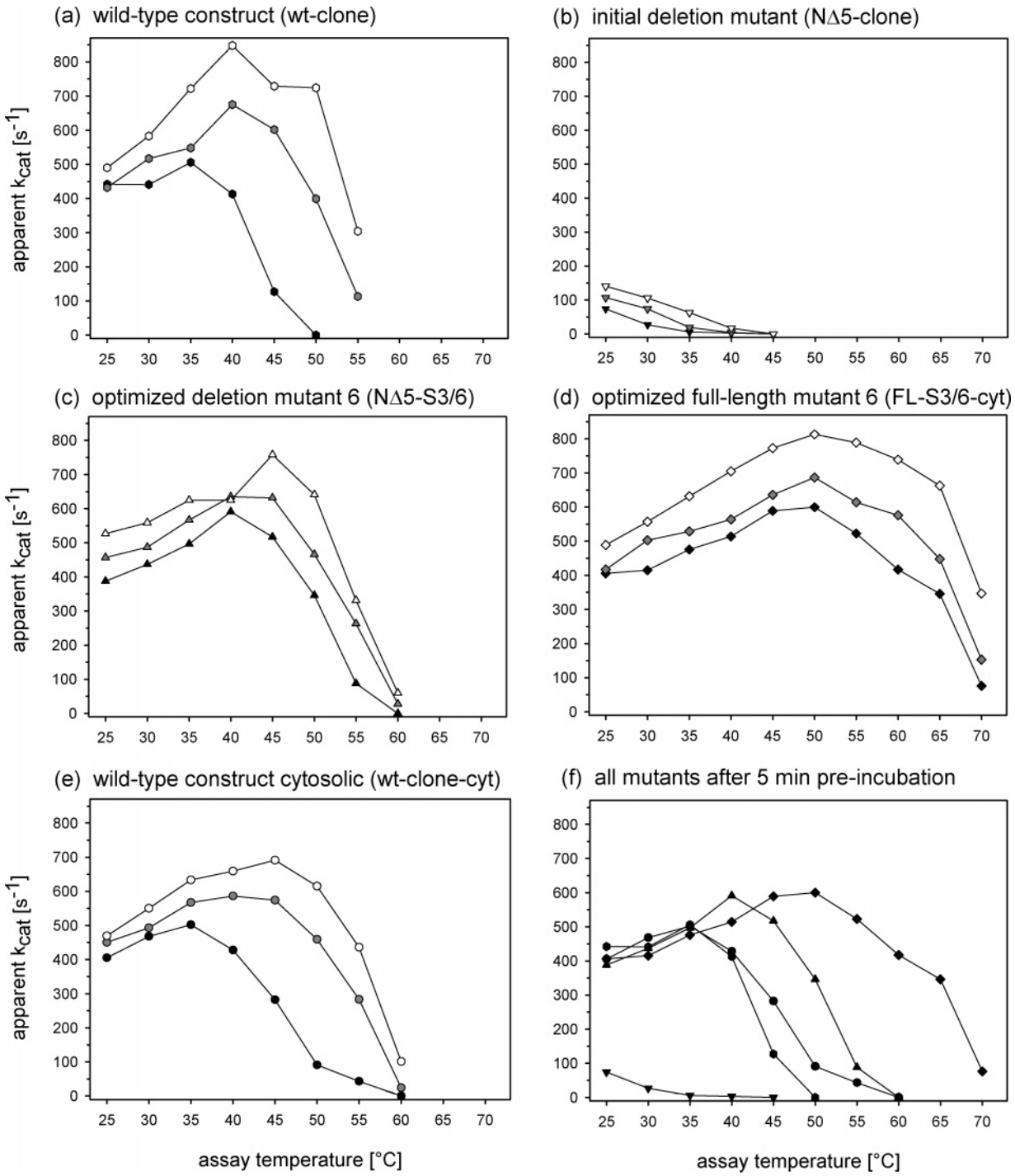

FIGURE 5: Temperature-dependent activity profiles of the investigated β-lactamase variants. (a−e) Thermoactivity profiles after various heat treatments. Apparent k_{cat} values were determined photospectrometrically at varying temperatures ranging from 25 to 70 °C using nitrocefin as a substrate. Diluted enzyme solutions (initial deletion mutant at 292 nM, all other mutants at 25 nM) were split into three fractions and subjected to different pretreatments: incubation for 5 min or 30 s at assay temperature (black and gray symbols, respectively), or storage on ice for 10 min (white symbols). Assay buffer (980 μL) was prewarmed in a heated water bath before reactions were started by adding enzyme solution (20 μL). Final enzyme concentrations were 5.9 nM for the initial deletion mutant and 0.5 nM for all other variants. (f) Summary of thermoactivity profiles obtained after preincubation for 5 min: (⬣) wt-clone (periplasmatic), (▼) NΔ5-clone, (▲) NΔ5-S3/6, (◆) FL-S3/6-cyt, and (●) wt-clone-cyt.

clones were nearly identical at assay temperatures up to 40 °C irrespective of pretreatment. At ≥50 °C, FL-S3/6-cyt retained significantly higher activities, especially under conditions of prolonged heat stress with a 5 min preincubation. The maximum catalytic activity of wt-clone-cyt was at 45 °C after ice incubation, but decreased to 35 °C following a 5 min preincubation. In contrast, the temperature optimum of FL-S3/6-cyt (50 °C) remained unchanged. Only the reaction rate decreased after heat incubation. Interestingly, the alterations between wt-clone and wt-clone-cyt at the N-terminus (Asp-Gly replaced with Met) influenced stability.

Comparison of the 5 min preincubation thermoactivity profiles of all truncated and full-length variants (Figure 5f) illustrates how terminal truncation diminished activity at 35−40 °C. Compensating amino acid substitutions restored activity and even improved stability. Re-extension of opti-

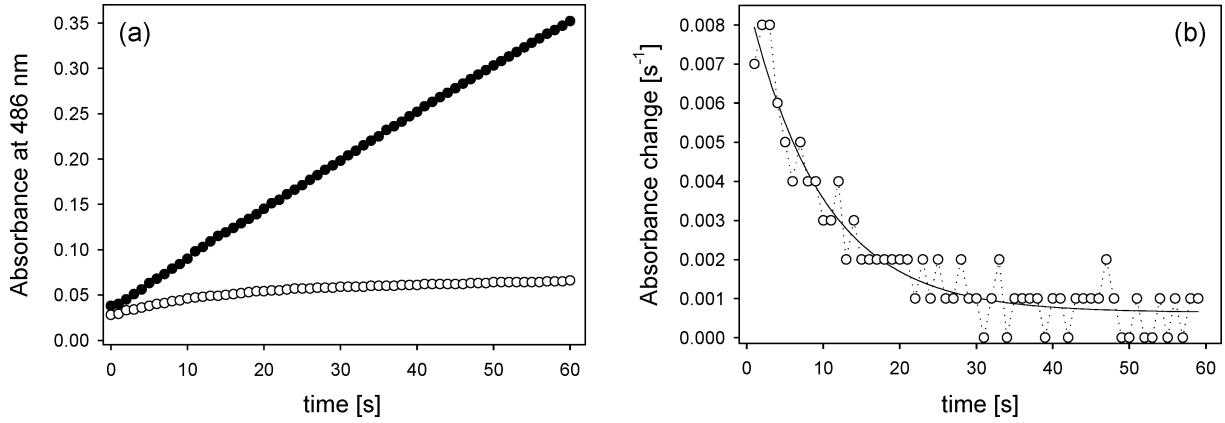

FIGURE 6: Enzyme kinetics and exponential decay of the catalytic activity of NΔ5-clone and stable kinetics of NΔ5-S3/6 at 40 °C. (a) Spectrophotometric analysis of product formation using the chromogenic substrate nitrocefin. The final enzyme concentration of NΔ5-clone (○) was 2.9 nM and of NΔ5-S3/6 (●) 0.5 nM. Twenty microliters of a concentrated enzyme solution was mixed with 980 μL of prewarmed assay buffer. (b) Exponential decay fit of enzymatic activity of NΔ5-clone using the change in absorbance per second ($\Delta A/\Delta t$) from the data shown in panel a. A three-parameter exponential decay fit using SigmaPlot revealed a half-life time of 7 s at 40 °C.

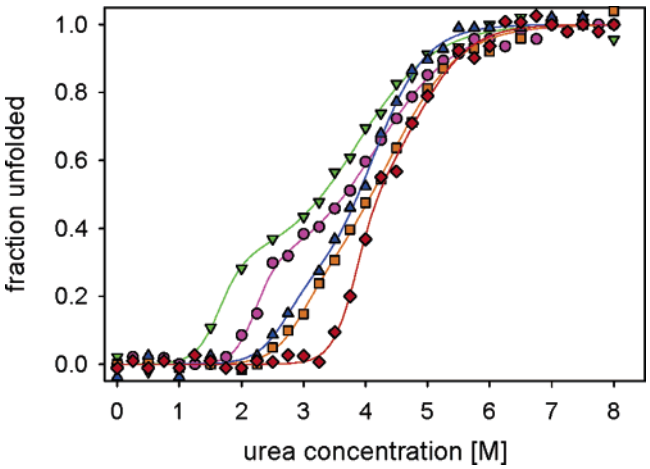

FIGURE 7: Urea-induced unfolding of β-lactamase variants. Denaturation was followed using the red shift of intrinsic fluorescence emission maxima. Enzyme samples [0.3−0.4 mM in 50 mM sodium phosphate and 150 mM NaCl (pH 7.2)] containing 0.25−8 M urea were equilibrated for 18−20 h at 19 °C and measured at 20−23 °C. Data were fitted assuming a three-state unfolding mechanism (lines): (green ▼) NΔ5-clone, (magenta ●) wt-clone-cyt, (orange ■) optimized deletion mutant NΔ5-S3/7, (blue ▲) mutant NΔ5-S3/6, and (red ◆) optimized full-length mutant FL-S3/6-cyt.

mized mutant S3/6 further increased thermostability as well as thermoactivity.

Urea-Induced Denaturation and Thermodynamic Stability. Next we tested the chemical stability of most constructs that were generated. The red shift of the intrinsic tryptophan fluorescence emission maximum as a function of urea concentration was monitored by fluorescence spectroscopy (Figure 7). The order of denaturation corresponded to the order seen in the thermoactivity assays. NΔ5-clone was the least stable followed by wt-clone-cyt. Optimized mutants NΔ5/S3-6 and NΔ5/S3-7 start to unfold at approximately the same urea concentration, and elongated FL/S3-6 is the last to unfold.

The unfolding showed a clear three-state behavior in the case of wt-clone-cyt and NΔ5-clone. Taking a closer look at the FL/S3-6-cyt data and comparing two- and three-state fits also strongly indicated a three-state behavior. The data of optimized mutants NΔ5/S3-6 and NΔ5/S3-7 could be explained by either two- or three-state unfolding. For comparison, all data were fitted using the three-state model N ⇌ I ⇌ U with eq 1, where N represents the native state, I the intermediate, and U the unfolded state (Table 3). This approach is supported by previously described intermediate folding states for TEM-type β-lactamases (*64*−*66*). Enzyme activity tests with urea-denatured proteins showed a decrease in activity upon first denaturation. The extracted thermodynamic values aid in the comparison and explanation of the obtained mutants but require careful interpretation due to underlying assumptions. The deletion of five N-terminal amino acids primarily affected the first transition, reducing the stability by ∼10 kJ/mol, and had little effect on the second transition. Optimizing for catalytic activity in vivo yielded clones displaying stabilization effects for both transitions, whereby the achieved stability of the first transition is below and the second above that of wt-clone. Elongation (clone FL/S3-6-cyt) considerably stabilized the first phase (19.6 kJ/mol compared to NΔ5/S3-6) but had little effect on the second transition (3.8 kJ/mol compared to NΔ5/S3-6). This is in agreement with the view that elongation compensated for truncation independent of the introduced mutations. Comparing FL-S3/6-cyt with wt-clone-cyt revealed a stabilization of 15 kJ/mol for the first and of 11.4 kJ/mol for the second transition. It is important to note that the optimized mutants denature at urea concentrations higher than that of wt-clone, confirming the stability ranking seen in thermoactivity assays.

DISCUSSION

Protein Truncation, Optimization, and Elongation. Stability of proteins is a general feature very important for biotechnological, industrial, and medical applications. Although major forces governing protein energetics are principally known, the generation and understanding of thermostable protein variants remain a challenging task. We used a truncation suppressor mutation approach (*34*) comprising the search for revertants or second site mutations of induced deletions. Focusing perturbation on termini, which are likely amenable to modifications, allowed us to decrease protein stability stepwise. Directed evolution determined how perturbations within a protein structure can be overcome by taking all residues into account without the bias of rational design. Combining compensating mutations with the full-

Table 3: Thermodynamic Parameters[a]

variant	$\Delta G°_{NI,H_2O}$ (kJ/mol)	m_{NI} (kJ mol^{-1} M^{-1})	$D^{1/2}_{NI}$ (M)	$\Delta G°_{IU,H_2O}$ (kJ/mol)	m_{IU} (kJ mol^{-1} M^{-1})	$D^{1/2}_{IU}$ (M)
wt-clone-cyt	30.4 ± 4.5	13.7 ± 2.1	2.9	15.8 ± 1.1	3.8 ± 0.2	4.2
NΔ5-clone	20.2 ± 5.5	12.3 ± 3.7	1.6	15.3 ± 1.7	3.9 ± 0.4	3.9
NΔ5-S3/7	27.1 ± 6.4	9.3 ± 2.6	2.9	19.0 ± 2.6	4.3 ± 0.5	4.4
NΔ5-S3/6	26.2 ± 10.1	9.8 ± 4.3	2.7	23.4 ± 3.2	5.7 ± 0.6	4.1
FL-S3/6-cyt	45.8 ± 7.7	11.9 ± 2.2	3.8	27.2 ± 7.0	5.6 ± 1.2	4.9

[a] Data were analyzed using the linear extrapolation method (*85*) assuming a biphasic unfolding transition (native, intermediate, and unfolded). The values for half-denaturation were obtained using eq 2.

length sequence revealed additive effects and little interdependence of missing and mutated residues. The data from mutant analysis have implications for understanding less conserved and terminal parts of a protein and, most important, for the understanding of stabilizing factors. A deletion−compensation approach may also help in identification of minimal structural requirements for a specific protein function in a different biological context or technical process.

Furthermore, β-lactamase is used for prodrug activation, making a stable lactamase a potential lead compound (*41*, *42*). Protein stability is important to ensure therapeutic efficacy particularly with regard to prolonged blood clearance times. In addition, a stable protein is a good starting point for optimizing activity toward certain prodrugs, thus broadening the scope for potentially useful prodrugs. In lactamase reporter assays, especially for genome wide screens, a reliably folding and stable enzyme might provide better signal-to-noise ratios (*45*, *46*). The quality of protein complementation assays might be further improved over the use of just the M182T mutation (*47*). Finding stabilizing mutations for lactamase could also aid in the prediction of future developments in pathogen resistance (*40*). β-Lactamase is a versatile model system due to the ready availability of several mutagenic studies (*43*, *67*) and crystal structures (*59*, *68*−*70*).

Structural Perturbation by Terminal Truncation. Four different truncation variants of β-lactamase, two from each end, provided impaired antibiotic resistance. Removal of five residues from the N-terminus of the β-lactamase construct decreased its thermostability significantly as demonstrated both in vivo and in vitro. Purified truncated protein exhibited a 6-fold decreased turnover number relative to that of the full-length wild-type variant and was rapidly inactivated above 25 °C with a half-life time of 7 s at 40 °C. Thermal instability of truncation mutant NΔ5 correlated with a high sensitivity to chemical denaturation. Urea-induced unfolding experiments detected a loss of conformational stability at 25 °C of ∼10 kJ/mol. Interestingly, the Michaelis constant of the deletion mutant approached values measured for the wild-type protein and the optimized variants, indicating that truncation affects primarily protein energetics and preserves nativelike active site architecture and enzyme−substrate interactions. In the case of β-lactamase, the complete polypeptide chain seems to be essential for specifying a sufficiently stable structural framework guiding efficient catalysis. The cooperative nature of stabilizing forces ensures that any perturbation even if distant from important functional regions readily transmits through the molecule, hence influencing also key positions with regard to stability or function. Our data corroborate the view that chain termini despite their high evolutionary sequence variability may contribute significantly to conformational stability (*35*, *37*) which may be harnessed, through truncation, to impose "mild" structural impairments compatible with folding.

Of course, it is conceivable that the truncation approach may not work smoothly in the case of one-chain multienzyme complexes. Even in some cases of smaller proteins, the removal of significant numbers of residues might be necessary. For example, truncation analysis of the monomeric 168-residue enzyme peptide deformylase showed that removal of 21 disordered residues of the C-terminus increased stability and only the deletion of 29 residues abolished activity (*71*). However, in general there is good evidence that progressive terminal truncation results in a stepwise reduction in thermostability and expression yields (*34*, *36*). Intermediate truncations likely fold to a loosely packed native structure (*37*), marking a perfect starting point for directed evolution and subsequent identification of second-site suppressors.

Distribution and Properties of Frequently Mutated Residues. Three rounds of directed evolution of NΔ5-clone selected with increasing concentrations of ampicillin generated variants with mutations compensating for the truncation. Table 1 lists amino acid substitutions of all sequenced clones isolated in the course of evolution. In total, 32 positions were mutated in a set of 34 sequenced clones. An extra backcrossing round of the obtained sequences with wt-clone was not carried out as for every position mutated in one clone (apart M182T) mutants with wild-type sequences at the respective position were also present in sufficient amounts to warrant the assumption that all present mutations are beneficial or at least neutral. This mutational scope is demonstrated by the T265M mutation present in all five analyzed second round clones but in only a few third round clones.

The minimal set of mutations required to rescue the heat-sensitive phenotype of the NΔ5 mutant was three (I84V, M182T, and A224V in clone S3/17), supporting the general view that minor amino acid changes are sufficient to change the stability of a protein significantly. The maximum number of substitutions found in a single optimized clone was 12 (clone S3/20), confirming the high tolerance of TEM-1 β-lactamase for amino acid exchanges. This is also indicated by a previous study randomizing all 263 codons of the TEM-1 gene with selection for the ability to confer wild-type levels of ampicillin resistance; 84% of all residues could be substituted without compromising in vivo functionality (*43*). None of the substitutions we found occurred at sites with an ascribed essential role in this previous study.

Approximately 19% of the mutations in our study were located at sites with low relative solvent accessibility (<20%) as calculated from PDB entry 1btl using What If (*72*). Only two mutated residues (I247V and T265M) had their side chains >95% buried (typical measure for specifying core residues) and were found in approximately one-third of all clones, suggesting that changes in the core did not overcome

adverse effects resulting from the loss of terminal interactions. This might also reflect the fact that core packing interactions are close to optimal, leaving little space for further improvements or at least requiring the coverage of broad sequence space to retrieve improved solutions. Hence, greater diversity might be necessary to find mutants with an optimized core. The majority of substitutions mapped to the surface or the boundary between core and surface. Approximately 40.5% of the mutations were located at sites with intermediate accessibility (>20%, <50%, classified as boundary), and 40.5% at sites with high accessibility (>50%, classified as surface). A straightforward analysis of surface substitutions and their stabilizing effects, however, is complicated as exposed residues generally contribute marginally to overall stability (*73*) but might also have a paramount beneficial impact (*74*, *75*).

The role of certain mutations might be further clarified by sequence comparison with natural and selected class A lactamases. Two substitutions, M182T and A224V, predominated in clones withstanding the highest ampicillin challenge (see Table 1). Comparison with 19 other class A β-lactamases (*60*) revealed a threonine at position 182 in 15 members and a serine in four members, indicating that a hydroxyl group might engage in important interactions at this site. At position 224, only TEM-1 shows an alanine, whereas three enzymes have a valine and 15 a glycine. Among the more frequently found substitutions are H153R, R120G, and I84V. The H153R mutation which we found in 11 of 26 of our third round clones was also found in a study permuting the lactamase structure and searching for stabilizing mutations (*76*). In the alignment of lactamases of Ambler et al., 14 of 20 lactamases carry an arginine at this position, and thus, H153R converts to consensus (*60*). In the alignment, position 120 which was mutated from arginine to glycine in nine of 26 clones is occupied by diverse residues with a slightly higher occurrence of Gly. In addition, the R120G mutation was also found in the permutation study (*76*). The I84V mutation found in 10 of 26 of our third round clones is one of the two mutations differentiating the TEM lactamase in pUC-derived plasmids from the pBR322-derived plasmids. The T265M exchange present in the five second round mutants analyzed was present in only 20% of the third round clones, ranking this mutation neutral (*77*).

Prevalent Substitutions Improve Interdomain Interactions. The M182T exchange is a well-known mutation found in a number of bacterial isolates resistant to frequently used inhibitors and cephalosporin antibiotics. In addition, it has been identified in several in vitro studies as a global suppressor of folding defects and impaired stability (*61*−*63*). Several TEM-1 variants carrying the M182T mutation have been crystallized (*40*, *63*), providing insight into the possible mechanism of stabilization. TEM-1 lactamase is a 263-residue protein consisting of two domains, an all-α domain formed by the central part of the chain (residues 69−212) and an α/β domain comprising the N- and C-terminal portions of the protein. The domains are connected by two hinge regions (residues 60−68 and 212−222). The hydroxyl group of Thr182 is thought to form additional H-bonds with the main chain carbonyl groups of Glu63 and Glu64 (*40*). The new H-bonds fall into a rigid part of the structure already featuring a network of interactions stabilizing the domain interface and active site. Thr181 and Phe66 form two H-bonds with each other via their backbone amides, and the hydroxyl group of Thr180 forms one H-bond to the guanidino group of the Arg65 moiety.

The second abundant substitution is A224V. Although the statistical basis of 26 sequenced third round clones does not justify the assumption that A224V is essential, it seems to play an important role. This is further supported by in vivo analysis of additional clones truncated by either 10 or 15 N-terminal residues carrying this mutation which do mediate resistance against ampicillin (data not shown). Ala224 resides on a short helical stretch (H10, residues 221−224) of an extended loop connecting helix H9 of the all-α domain and β-strand S3 of the α/β domain. This residue is located adjacent to Arg222 which stabilizes the loop by forming a salt bridge with Asp233. The side chain of Ala224 is near a hydrophobic region that includes the side chains of Ala280, Ala284, and Ile287 from the C-terminal helix, but hardly makes any contact. The side chains of all residues involved in this hydrophobic cluster have *B*-factors similar to those of fully buried residues in the TEM1 structure, indicating a well-defined local conformation suited to supporting strong interactions. The larger size and higher hydrophobicity of the valine relative to those of the alanine side chain may enhance hydrophobic interactions and van der Waals contacts to side chains of the above-mentioned hydrophobic cluster, thereby enforcing linkage of the two domains. Stabilizing hydrophobic interactions close to the protein surface have been demonstrated for the thermolysin-like neutral protease (*75*). Both mutations (M182T and A224V) are likely key to small clusters of "multivalent" interactions at an atomic scale which significantly exceed the sum of the individual constituents. We speculate that the A224V mutation has not yet been identified in natural isolates (see http://www.lahey.org/studies) or by directed evolution of broad spectrum lactamases (*40*), because it is less compatible with the catalysis of certain substrates. However, this mutation in combination with more than one spectrum broadening mutation might pose a future threat.

Interestingly, the two substitutions present in all clones are located in loop regions which in general are susceptible to local unfolding (*78*) and therefore are thought to initiate the process of denaturation. These so-called unfolding regions (*79*) are usually identified by mutagenesis or immobilization studies requiring time-consuming construction and characterization of many mutants. The truncation−compensation approach simplified the identification of such unfolding regions and, at the same time, provided sets of stabilizing substitutions.

Three-State Unfolding. A clear three-state unfolding behavior was observed for NΔ5-clone and wt-clone. Intermediate folding states for TEM-1 and TEM-2 (differs from TEM-1 by a single Q39K substitution) have been described previously (*64*−*66*). However, in these cases, the intermediate was only observed in activity measurements or CD spectra, not using intrinsic tryptophan fluorescence. The obvious intermediates in our denaturation curves are likely the result of the additional amino acids at the N- and C-termini, which destabilize the protein as seen in the activity assays. The destabilization leads to a more pronounced intermediate as detected by the tryptophan environment, which is again camouflaged with increasing stability of the optimized mutants.

Compensating Substitutions Dramatically Increase the Thermal and Chemical Stability of the Full-Length Enzyme. Temperature−activity assays demonstrated a dramatically augmented thermostability of the optimized full-length enzyme relative to the wild-type (Figure 6f). Thus, amino acid exchanges that rescued thermosensitive enzymes also provided additional stabilization in the full-length context. It is important to note that the stabilization that was obtained is beyond what could have been selected starting with wild-type lactamase since the stabilized full-length mutant confers resistance to only small amounts of antibiotic. Considering activity assays of crude cell extracts, weakened signal sequence cleavage, and the purification of active mutants with signal sequence, we propose that a major contribution to this finding is the folding of a significant fraction of this mutant in the cytosol which is consequently not transported to the periplasm to inactivate ampicillin. In addition, a slightly lower expression level in combination with a lower catalytic efficiency could also contribute to the reduced resistance.

Stabilizing effects after truncation have also been demonstrated for C-terminal deletion mutants of ribonuclease HI (*34*). Before the advent of directed evolution, the authors of the latter study pointed to the potential use of terminal truncation in combination with random mutagenesis in identifying stabilizing mutations. In a further study, structural perturbations were introduced by replacing 20% of a thermophilic protein with the corresponding regions of a mesophilic homologue. Random mutagenesis and metabolic selection in a thermophilic host enhanced the thermostability of an already stable enzyme (*80*). Another study demonstrated that mutations found by directed evolution to compensate for missing disulfide bridges in an antibody fragment further stabilized cysteine-restored mutants (*81*). Selection in a thermophilic organism demands additional expertise and equipment, and the removal of disulfide bridges is limited to proteins bearing this stabilizing feature. In conclusion, structural perturbation is a very general method, and terminal truncation is in most cases the easiest route for imposing stepwise perturbations. In combination with directed evolution, this simple yet rather efficient approach can create thermostable enzymes and promote our understanding of thermostability.

ACKNOWLEDGMENT

We thank Katja M. Arndt for helpful discussions and critically reading the manuscript, Susanne Knall for help with some experiments, and Jody Mason for reading the manuscript.

REFERENCES

1. Jaenicke, R., and Böhm, G. (1998) The stability of proteins in extreme environments, *Curr. Opin. Struct. Biol. 8*, 738−748.
2. Ladenstein, R., and Antranikian, G. (1998) Proteins from hyperthermophiles: Stability and enzymatic catalysis close to the boiling point of water, *Adv. Biochem. Eng. Biotechnol. 61*, 37−85.
3. Querol, E., Perez-Pons, J. A., and Mozo-Villarias, A. (1996) Analysis of protein conformational characteristics related to thermostability, *Protein Eng. 9*, 265−271.
4. Sterner, R., and Liebl, W. (2001) Thermophilic adaptation of proteins, *Crit. Rev. Biochem. Mol. Biol. 36*, 39−106.
5. Vieille, C., and Zeikus, G. J. (2001) Hyperthermophilic enzymes: Sources, uses, and molecular mechanisms for thermostability, *Microbiol. Mol. Biol. Rev. 65*, 1−43.
6. Wray, J. W., Baase, W. A., Lindstrom, J. D., Weaver, L. H., Poteete, A. R., and Matthews, B. W. (1999) Structural analysis of a non-contiguous second-site revertant in T4 lysozyme shows that increasing the rigidity of a protein can enhance its stability, *J. Mol. Biol. 292*, 1111−1120.
7. Otzen, D. E., Rheinnecker, M., and Fersht, A. R. (1995) Structural factors contributing to the hydrophobic effect: The partly exposed hydrophobic minicore in chymotrypsin inhibitor 2, *Biochemistry 34*, 13051−13058.
8. Akasako, A., Haruki, M., Oobatake, M., and Kanaya, S. (1997) Conformational stabilities of *Escherichia coli* RNase HI variants with a series of amino acid substitutions at a cavity within the hydrophobic core, *J. Biol. Chem. 272*, 18686−18693.
9. Ohmura, T., Ueda, T., Ootsuka, K., Saito, M., and Imoto, T. (2001) Stabilization of hen egg white lysozyme by a cavity-filling mutation, *Protein Sci. 10*, 313−320.
10. Matsumura, M., Becktel, W. J., and Matthews, B. W. (1988) Hydrophobic stabilization in T4 lysozyme determined directly by multiple substitutions of Ile 3, *Nature 334*, 406−410.
11. Vlassi, M., Cesareni, G., and Kokkinidis, M. (1999) A correlation between the loss of hydrophobic core packing interactions and protein stability, *J. Mol. Biol. 285*, 817−827.
12. Kannan, N., and Vishveshwara, S. (2000) Aromatic clusters: A determinant of thermal stability of thermophilic proteins, *Protein Eng. 13*, 753−761.
13. Hennig, M., Darimont, B., Sterner, R., Kirschner, K., and Jansonius, J. N. (1995) 2.0 Å structure of indole-3-glycerol phosphate synthase from the hyperthermophile *Sulfolobus solfataricus*: Possible determinants of protein stability, *Structure 3*, 1295−1306.
14. Iwai, H., and Plückthun, A. (1999) Circular β-lactamase: Stability enhancement by cyclizing the backbone, *FEBS Lett. 459*, 166−172.
15. Pace, C. N., Grimsley, G. R., Thomson, J. A., and Barnett, B. J. (1988) Conformational stability and activity of ribonuclease T1 with zero, one, and two intact disulfide bonds, *J. Biol. Chem. 263*, 11820−11825.
16. Arnold, F. H., and Zhang, J. H. (1994) Metal-mediated protein stabilization, *Trends Biotechnol. 12*, 189−192.
17. Serrano, L., and Fersht, A. R. (1989) Capping and α-helix stability, *Nature 342*, 296−299.
18. Thompson, M. J., and Eisenberg, D. (1999) Transproteomic evidence of a loop-deletion mechanism for enhancing protein thermostability, *J. Mol. Biol. 290*, 595−604.
19. Matthews, B. W., Nicholson, H., and Becktel, W. J. (1987) Enhanced protein thermostability from site-directed mutations that decrease the entropy of unfolding, *Proc. Natl. Acad. Sci. U.S.A. 84*, 6663−6667.
20. Karshikoff, A., and Ladenstein, R. (2001) Ion pairs and the thermotolerance of proteins from hyperthermophiles: A "traffic rule" for hot roads, *Trends Biochem. Sci. 26*, 550−556.
21. Szilagyi, A., and Zavodszky, P. (2000) Structural differences between mesophilic, moderately thermophilic and extremely thermophilic protein subunits: Results of a comprehensive survey, *Structure 8*, 493−504.
22. Vogt, G., Woell, S., and Argos, P. (1997) Protein thermal stability, hydrogen bonds, and ion pairs, *J. Mol. Biol. 269*, 631−643.
23. Petsko, G. A. (2001) Structural basis of thermostability in hyperthermophilic proteins, or "there's more than one way to skin a cat", *Methods Enzymol. 334*, 469−478.
24. Malakauskas, S. M., and Mayo, S. L. (1998) Design, structure and stability of a hyperthermophilic protein variant, *Nat. Struct. Biol. 5*, 470−475.
25. Filikov, A. V., Hayes, R. J., Luo, P., Stark, D. M., Chan, C., Kundu, A., and Dahiyat, B. I. (2002) Computational stabilization of human growth hormone, *Protein Sci. 11*, 1452−1461.
26. Lehmann, M., Loch, C., Middendorf, A., Studer, D., Lassen, S. F., Pasamontes, L., van Loon, A. P., and Wyss, M. (2002) The consensus concept for thermostability engineering of proteins: Further proof of concept, *Protein Eng. 15*, 403−411.
27. Stemmer, W. P. (1994) Rapid evolution of a protein in vitro by DNA shuffling, *Nature 370*, 389−391.
28. Stemmer, W. P. (1994) DNA shuffling by random fragmentation and reassembly: In vitro recombination for molecular evolution, *Proc. Natl. Acad. Sci. U.S.A. 91*, 10747−10751.
29. Petrounia, I. P., and Arnold, F. H. (2000) Designed evolution of enzymatic properties, *Curr. Opin. Biotechnol. 11*, 325−330.

30. Santos, J., Gebhard, L. G., Risso, V. A., Ferreyra, R. G., Rossi, J. P., and Ermacora, M. R. (2004) Folding of an abridged β-lactamase, *Biochemistry 43*, 1715−1723.
31. Lehmann, M., Kostrewa, D., Wyss, M., Brugger, R., D'Arcy, A., Pasamontes, L., and van Loon, A. P. (2000) From DNA sequence to improved functionality: Using protein sequence comparisons to rapidly design a thermostable consensus phytase, *Protein Eng. 13*, 49−57.
32. Steipe, B., Schiller, B., Plückthun, A., and Steinbacher, S. (1994) Sequence statistics reliably predict stabilizing mutations in a protein domain, *J. Mol. Biol. 240*, 188−192.
33. Sherwood, L. M., and Potts, J. T., Jr. (1965) Conformational studies of pancreatic ribonuclease and its subtilisin-produced derivatives, *J. Biol. Chem. 240*, 3799−3805.
34. Haruki, M., Noguchi, E., Akasako, A., Oobatake, M., Itaya, M., and Kanaya, S. (1994) A novel strategy for stabilization of *Escherichia coli* ribonuclease HI involving a screen for an intragenic suppressor of carboxyl-terminal deletions, *J. Biol. Chem. 269*, 26904−26911.
35. Yang, F., Cheng, Y., Peng, J., Zhou, J., and Jing, G. (2001) Probing the conformational state of a truncated staphylococcal nuclease R using time of flight mass spectrometry with limited proteolysis, *Eur. J. Biochem. 268*, 4227−4232.
36. Trevino, R. J., Tsalkova, T., Kramer, G., Hardesty, B., Chirgwin, J. M., and Horowitz, P. M. (1998) Truncations at the NH2 terminus of rhodanese destabilize the enzyme and decrease its heterologous expression, *J. Biol. Chem. 273*, 27841−27847.
37. Trevino, R. J., Gliubich, F., Berni, R., Cianci, M., Chirgwin, J. M., Zanotti, G., and Horowitz, P. M. (1999) NH2-terminal sequence truncation decreases the stability of bovine rhodanese, minimally perturbs its crystal structure, and enhances interaction with GroEL under native conditions, *J. Biol. Chem. 274*, 13938−13947.
38. Vainshtein, I., Atrazhev, A., Eom, S. H., Elliott, J. F., Wishart, D. S., and Malcolm, B. A. (1996) Peptide rescue of an N-terminal truncation of the Stoffel fragment of taq DNA polymerase, *Protein Sci. 5*, 1785−1792.
39. Van der Schueren, J., Robben, J., and Volckaert, G. (1998) Misfolding of chloramphenicol acetyltransferase due to carboxy-terminal truncation can be corrected by second-site mutations, *Protein Eng. 11*, 1211−1217.
40. Orencia, M. C., Yoon, J. S., Ness, J. E., Stemmer, W. P., and Stevens, R. C. (2001) Predicting the emergence of antibiotic resistance by directed evolution and structural analysis, *Nat. Struct. Biol. 8*, 238−242.
41. Rodrigues, M. L., Presta, L. G., Kotts, C. E., Wirth, C., Mordenti, J., Osaka, G., Wong, W. L., Nuijens, A., Blackburn, B., and Carter, P. (1995) Development of a humanized disulfide-stabilized anti-p185HER2 Fv-β-lactamase fusion protein for activation of a cephalosporin doxorubicin prodrug, *Cancer Res. 55*, 63−70.
42. Cortez-Retamozo, V., Backmann, N., Senter, P. D., Wernery, U., De Baetselier, P., Muyldermans, S., and Revets, H. (2004) Efficient cancer therapy with a nanobody-based conjugate, *Cancer Res. 64*, 2853−2857.
43. Huang, W., Petrosino, J., Hirsch, M., Shenkin, P. S., and Palzkill, T. (1996) Amino acid sequence determinants of β-lactamase structure and activity, *J. Mol. Biol. 258*, 688−703.
44. Doucet, N., De Wals, P. Y., and Pelletier, J. N. (2004) Site-saturation mutagenesis of Tyr-105 reveals its importance in substrate stabilization and discrimination in TEM-1 β-lactamase, *J. Biol. Chem. 279*, 46295−46303.
45. Zlokarnik, G., Negulescu, P. A., Knapp, T. E., Mere, L., Burres, N., Feng, L., Whitney, M., Roemer, K., and Tsien, R. Y. (1998) Quantitation of transcription and clonal selection of single living cells with β-lactamase as reporter, *Science 279*, 84−88.
46. Whitney, M., Rockenstein, E., Cantin, G., Knapp, T., Zlokarnik, G., Sanders, P., Durick, K., Craig, F. F., and Negulescu, P. A. (1998) A genome-wide functional assay of signal transduction in living mammalian cells, *Nat. Biotechnol. 16*, 1329−1333.
47. Galarneau, A., Primeau, M., Trudeau, L. E., and Michnick, S. W. (2002) β-Lactamase protein fragment complementation assays as in vivo and in vitro sensors of protein protein interactions, *Nat. Biotechnol. 20*, 619−622.
48. Wehrman, T., Kleaveland, B., Her, J. H., Balint, R. F., and Blau, H. M. (2002) Protein−protein interactions monitored in mammalian cells via complementation of β-lactamase enzyme fragments, *Proc. Natl. Acad. Sci. U.S.A. 99*, 3469−3474.
49. Yanisch-Perron, C., Vieira, J., and Messing, J. (1985) Improved M13 phage cloning vectors and host strains: Nucleotide sequences of the M13mp18 and pUC19 vectors, *Gene 33*, 103−119.
50. Lei, S. P., Lin, H. C., Wang, S. S., Callaway, J., and Wilcox, G. (1987) Characterization of the *Erwinia carotovora* pelB gene and its product pectate lyase, *J. Bacteriol. 169*, 4379−4383.
51. Krebber, A., Bornhauser, S., Burmester, J., Honegger, A., Willuda, J., Bosshard, H. R., and Plückthun, A. (1997) Reliable cloning of functional antibody variable domains from hybridomas and spleen cell repertoires employing a reengineered phage display system, *J. Immunol. Methods 201*, 35−55.
52. Olins, P. O., Devine, C. S., Rangwala, S. H., and Kavka, K. S. (1988) The T7 phage gene 10 leader RNA, a ribosome-binding site that dramatically enhances the expression of foreign genes in *Escherichia coli*, *Gene 73*, 227−235.
53. Thomas, M. R. (1994) Simple, effective cleanup of DNA ligation reactions prior to electro-transformation of *E. coli*, *BioTechniques 16*, 988−990.
54. Gill, S., and von Hippel, G. (1989) Calculation of protein extinction coefficients from amino acid sequence data, *Anal. Biochem. 182*, 319−326.
55. Sigal, I. S., DeGrado, W. F., Thomas, B. J., and Petteway, S. R., Jr. (1984) Purification and properties of thiol β-lactamase. A mutant of pBR322 β-lactamase in which the active site serine has been replaced with cysteine, *J. Biol. Chem. 259*, 5327−5332.
56. Barrick, D., and Baldwin, R. L. (1993) Three-state analysis of sperm whale apomyoglobin folding, *Biochemistry 32*, 3790−3796.
57. Pace, C. N. (1986) Determination and analysis of urea and guanidine hydrochloride denaturation curves, *Methods Enzymol. 131*, 266−280.
58. Vanhove, M., Houba, S., Lamotte-Brasseur, J., and Frere, J. M. (1995) Probing the determinants of protein stability: Comparison of class A β-lactamases, *Biochem. J. 308* (Part 3), 859−864.
59. Jelsch, C., Mourey, L., Masson, J. M., and Samama, J. P. (1993) Crystal structure of *Escherichia coli* TEM1 β-lactamase at 1.8 Å resolution, *Proteins 16*, 364−383.
60. Ambler, R. P., Coulson, A. F., Frere, J. M., Ghuysen, J. M., Joris, B., Forsman, M., Levesque, R. C., Tiraby, G., and Waley, S. G. (1991) A standard numbering scheme for the class A β-lactamases, *Biochem. J. 276* (Part 1), 269−270.
61. Sideraki, V., Huang, W., Palzkill, T., and Gilbert, H. F. (2001) A secondary drug resistance mutation of TEM-1 β-lactamase that suppresses misfolding and aggregation, *Proc. Natl. Acad. Sci. U.S.A. 98*, 283−288.
62. Huang, W., and Palzkill, T. (1997) A natural polymorphism in β-lactamase is a global suppressor, *Proc. Natl. Acad. Sci. U.S.A. 94*, 8801−8806.
63. Wang, X., Minasov, G., and Shoichet, B. K. (2002) Evolution of an antibiotic resistance enzyme constrained by stability and activity trade-offs, *J. Mol. Biol. 320*, 85−95.
64. Frech, C., Wunderlich, M., Glockshuber, R., and Schmid, F. X. (1996) Competition between DsbA-mediated oxidation and conformational folding of RTEM1 β-lactamase, *Biochemistry 35*, 11386−11395.
65. Vanhove, M., Raquet, X., and Frere, J. M. (1995) Investigation of the folding pathway of the TEM-1 β-lactamase, *Proteins 22*, 110−118.
66. Zahn, R., Axmann, S. E., Rucknagel, K. P., Jaeger, E., Laminet, A. A., and Plückthun, A. (1994) Thermodynamic partitioning model for hydrophobic binding of polypeptides by GroEL. I. GroEL recognizes the signal sequences of β-lactamase precursor, *J. Mol. Biol. 242*, 150−164.
67. Plückthun, A., and Knowles, J. R. (1987) The consequences of stepwise deletions from the signal-processing site of β-lactamase, *J. Biol. Chem. 262*, 3951−3957.
68. Herzberg, O. (1991) Refined crystal structure of β-lactamase from *Staphylococcus aureus* PC1 at 2.0 Å resolution, *J. Mol. Biol. 217*, 701−719.
69. Moews, P. C., Knox, J. R., Dideberg, O., Charlier, P., and Frere, J. M. (1990) β-Lactamase of *Bacillus licheniformis* 749/C at 2 Å resolution, *Proteins 7*, 156−171.
70. Strynadka, N. C., Adachi, H., Jensen, S. E., Johns, K., Sielecki, A., Betzel, C., Sutoh, K., and James, M. N. (1992) Molecular structure of the acyl-enzyme intermediate in β-lactam hydrolysis at 1.7 Å resolution, *Nature 359*, 700−705.
71. Meinnel, T., Lazennec, C., Dardel, F., Schmitter, J. M., and Blanquet, S. (1996) The C-terminal domain of peptide deformylase is disordered and dispensable for activity, *FEBS Lett. 385*, 91−95.

72. Vriend, G. (1990) WHAT IF: A molecular modeling and drug design program, *J. Mol. Graphics 8*, 29−32, 52−56.
73. Bowie, J. U., Reidhaar-Olson, J. F., Lim, W. A., and Sauer, R. T. (1990) Deciphering the message in protein sequences: Tolerance to amino acid substitutions, *Science 247*, 1306−1310.
74. Martin, A., Sieber, V., and Schmid, F. X. (2001) In-vitro selection of highly stabilized protein variants with optimized surface, *J. Mol. Biol. 309*, 717−726.
75. Van den Burg, B., Dijkstra, B. W., Vriend, G., Van der Vinne, B., Venema, G., and Eijsink, V. G. (1994) Protein stabilization by hydrophobic interactions at the surface, *Eur. J. Biochem. 220*, 981−985.
76. Osuna, J., Perez-Blancas, A., and Soberon, X. (2002) Improving a circularly permuted TEM-1 β-lactamase by directed evolution, *Protein Eng. 15*, 463−470.
77. Huang, W., Le, Q. Q., LaRocco, M., and Palzkill, T. (1994) Effect of threonine-to-methionine substitution at position 265 on structure and function of TEM-1 β-lactamase, *Antimicrob. Agents Chemother. 38*, 2266−2269.
78. Daggett, V., and Levitt, M. (1993) Protein unfolding pathways explored through molecular dynamics simulations, *J. Mol. Biol. 232*, 600−619.
79. Mansfeld, J., Vriend, G., Van den Burg, B., Eijsink, V. G., and Ulbrich-Hofmann, R. (1999) Probing the unfolding region in a thermolysin-like protease by site-specific immobilization, *Biochemistry 38*, 8240−8245.
80. Kotsuka, T., Akanuma, S., Tomuro, M., Yamagishi, A., and Oshima, T. (1996) Further stabilization of 3-isopropylmalate dehydrogenase of an extreme thermophile, *Thermus thermophilus*, by a suppressor mutation method, *J. Bacteriol. 178*, 723−727.
81. Wörn, A., and Plückthun, A. (1998) Mutual stabilization of VL and VH in single-chain antibody fragments, investigated with mutants engineered for stability, *Biochemistry 37*, 13120−13127.
82. Shindyalov, I. N., and Bourne, P. E. (1998) Protein structure alignment by incremental combinatorial extension (CE) of the optimal path, *Protein Eng. 11*, 739−747.
83. Sayle, R. A., and Milner-White, E. J. (1995) RASMOL: Biomolecular graphics for all, *Trends Biochem. Sci. 20*, 374.
84. Guex, N., and Peitsch, M. C. (1997) SWISS-MODEL and the Swiss-PdbViewer: An environment for comparative protein modeling, *Electrophoresis 18*, 2714−2723.
85. Santoro, M. M., and Bolen, D. W. (1988) Unfolding free energy changes determined by the linear extrapolation method. 1. Unfolding of phenylmethanesulfonyl α-chymotrypsin using different denaturants, *Biochemistry 27*, 8063−8068.

BI0501885